Nuclear Materials and Energy 000 (2016) 1–5

Contents lists available at ScienceDirect

Nuclear Materials and Energy

journal homepage: www.elsevier.com/locate/nme

Influence of the C content on the permeation of hydrogen in Fe alloys with low contents of C

I. Peñalva[a,*], G. Alberro[a], F. Legarda[a], C.J. Ortiz[b], R. Vila[b]

[a] University of the Basque Country (UPV/EHU), Department of Nuclear Engineering & Fluid Mechanics, Faculty of Engineering, Alda. Urquijo s/n, 48013 Bilbao, Spain
[b] CIEMAT, Avda. Complutense 22, 28040 Madrid, Spain

ARTICLE INFO

Article history:
Received 16 November 2015
Revised 5 February 2016
Accepted 13 February 2016
Available online xxx

Keywords:
Permeability
Hydrogen
Tritium
Iron alloy

ABSTRACT

In this work, the permeability of hydrogen through samples of six Fe alloys was experimentally analyzed. The main objective of this work was to determine the influence of the C content of the alloy in the permeability of hydrogen. Three of the samples, pure Fe, FeP and Fe10%Cr, contained negligible quantities of C, whereas the other three, FeC, FePC, and Fe10%CrC, had the same metallurgical composition as their corresponding pair, with the only difference in the carbon content. The gas evolution permeation technique was used to measure the hydrogen transport parameter of permeability in these alloys. The experimental measurements were carried out with temperatures ranging from 423 K to 823 K and for high purity hydrogen loading pressures ranging from 1.0×10^3 Pa to 1.5×10^5 Pa.

The experimental permeation results were analyzed using a non-linear least square fitting. The final resulting values of the permeability were paired off in order to determine the effect of the C content: pure Fe versus FeC, FeP versus FePC and Fe10%Cr versus Fe10%CrC. According to the results, the influence of the metallurgical composition of C in Fe alloys on the permeability of hydrogen is discussed together with the synergistic effects caused by the presence of P and Cr.

1. Introduction

Ferritic-martensitic steels are candidate materials for blanket structural components that will constitute the future thermonuclear fusion devices. They have favorable thermo-mechanical properties and they can withstand high neutron irradiation and temperature ranges. In addition, they have the potential for reduced or even low-neutron induced activation [1–6].

However, the tritium inventory that is retained in different components of the reactor together with the ability of tritium to migrate through the walls of any material to personnel affected regions, may affect to the operation of a fusion reactor [7–9]. Therefore, the transport parameters of hydrogen isotopes (protium, deuterium and tritium) through the materials used for the plasma facing components are fundamental for the final design of a fusion reactor [10,11]. These transport parameters of hydrogen depend on the different metallurgical components of the Fe alloys [12–16].

In this work, the experimental gas permeation technique was used to characterize the hydrogen permeability in six different Fe alloys provided by the European Fusion Development Agreement (EFDA) with controlled chemical alloying elements and microstructure [17]: pure Fe metal, FeC alloy, FeP alloy, FePC alloy, Fe10%Cr alloy and Fe10%CrC alloy (see Table 1). The experimental results allow the analysis of the influence that the alloying element C has on the permeability of hydrogen for Fe alloys.

2. Material

The alloys were provided as cylindrical rods of 10.9 mm diameter each. As long as the assembly of the permeation column requires a thin slice of material, the original cylinders were cut in small disks. This work was carried out by CIEMAT. A cutoff machine with diamond disks was used to cut the samples to a thickness of about 1.3 mm. Then, a grinding sequence begins with 320-grit papers and then using progressively finer abrasive grits (600, 1200 and 4000) with the sample fixed in a cylinder glass with paraffin. During the polishing step, the specimens are polished with diamond paste (3, 1 and ¼ μm) in a napped cloth. By heating at 353 K, the sample is removed from the cylinder glass

* Corresponding author. Tel.: +34946014277.
E-mail address: igor.penalva@ehu.eus (I. Peñalva).

http://dx.doi.org/10.1016/j.nme.2016.02.004

Table 1
Chemical alloying elements and microstructure of the tested samples provided by EFDA [5].

Material		Composition [wt. ppm]						Grain size [μm]			Thickness [mm]
		C	S	O	N	P	Cr	min	Average	max	
Pure Fe		4	2	4	1	< 5	< 2	4	183	650	0.57
FeC		48	2	2	1	< 5	< 2	5	265	786	0.18
FeP	Centre	3	3	3	1	89	< 2	2	55	227	1.06
	Near the surface								118	475	
FePC	Centre	45–46	3	2	1	88	< 2	2	76–107	287	0.97
	Near the surface	33–35							139	374	
Fe10%Cr		4	4	4	3	< 5	10.10 wt%	3	82	259	1.30
Fe10%CrC		820	2	2	3	< 5	10.10 wt%	Not concerned			1.01

before the cleaning procedure takes place: ultrasonic bath with acetone, cleaning with soap and water and final ultrasonic bath with ethanol. The sample is then dried in hot air and, once in the permeation column heated up to 823 K under ultra-high vacuum (UHV) conditions. The final thicknesses of the tested samples are shown in Table 1.

3. Experimental

The permeability of H through the samples was measured by means of gas evolution permeation technique [14-16] (see Fig. 1). The recording of the pressure increase due to the gas flux that passes through a thin membrane of the material from a constant high gas pressure (p_h) region to a low-pressure region at initial UHV conditions is the basis of this experimental technique. This measurement of the pressure increase is made by means of two capacitance manometers (Baratron MKS-Instr USA), P1 and P2 with full scale range of 1000 Pa and 13.33 Pa, respectively. Fig. 2 shows a typical permeation signal obtained for FePC alloy at 475 °C with a loading pressure of 1.5 bar. The mathematical analysis of the steady-state permeation flux allows the precise evaluation of the permeability under diffusion-limited regimes.

The temperature of the sample is measured by a Ni–Cr/Ni thermocouple inserted into a well drilled in one of the two flanges of the permeation column. This temperature is fixed by means of an electrical resistance furnace (F) regulated by a PID controller. The pressure controller (PC) is responsible for the control of the pressure of the high-pressure face of the specimen to any desired gas driving pressure, which is measured by means of a high-pressure transducer (HPT).

There are three ultra-high vacuum pumping units, UHV, that pump down the inner volumes of the rig to the desired vacuum level. Three Penning gauges PG in different zones of the facility check the vacuum state and a quadrupole mass spectrometer (QMS) is available to check the purity of the gas and the vacuum level. Before every experimental test with high purity hydrogen

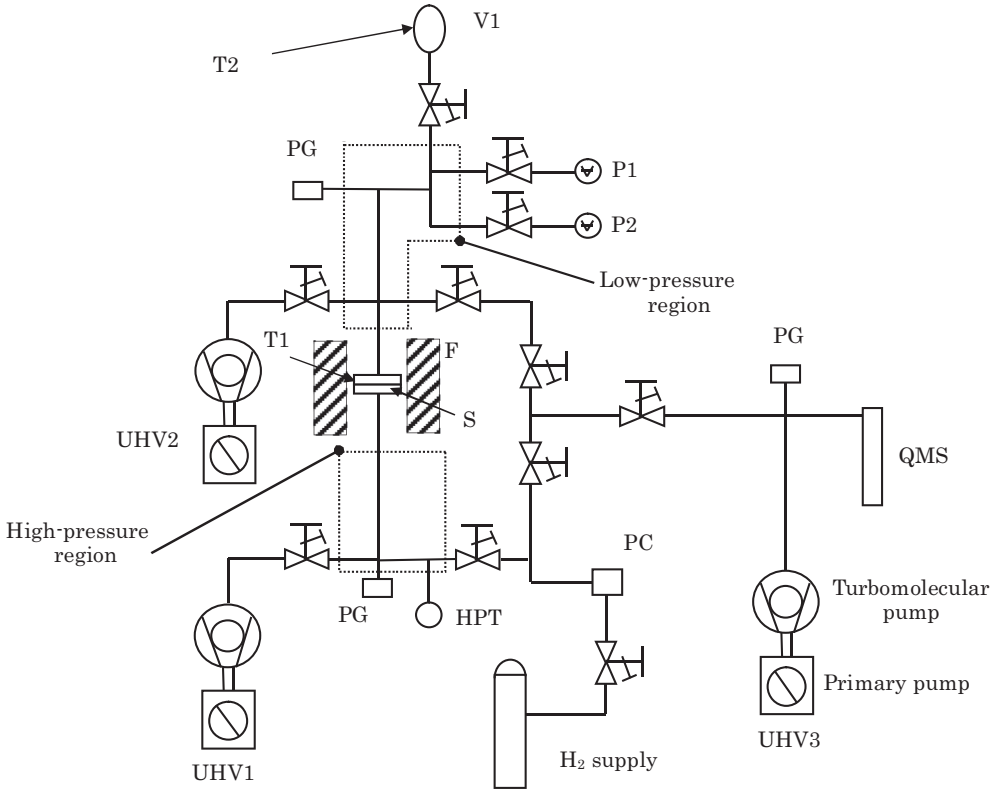

Fig. 1. Schematic view of the permeation facility. PG, Penning gauge; F, furnace; PC, pressure controller; HPT, high-pressure transducer; QMS, quadrupole mass spectrometer; S, specimen; T1, T2, Ni/Cr–Ni thermocouples; P1, P2, capacitance manometers; UHV, ultra-high vacuum pumping units; V1, calibrated volume.

Please cite this article as: I. Peñalva et al., Influence of the C content on the permeation of hydrogen in Fe alloys with low contents of C, Nuclear Materials and Energy (2016), http://dx.doi.org/10.1016/j.nme.2016.02.004

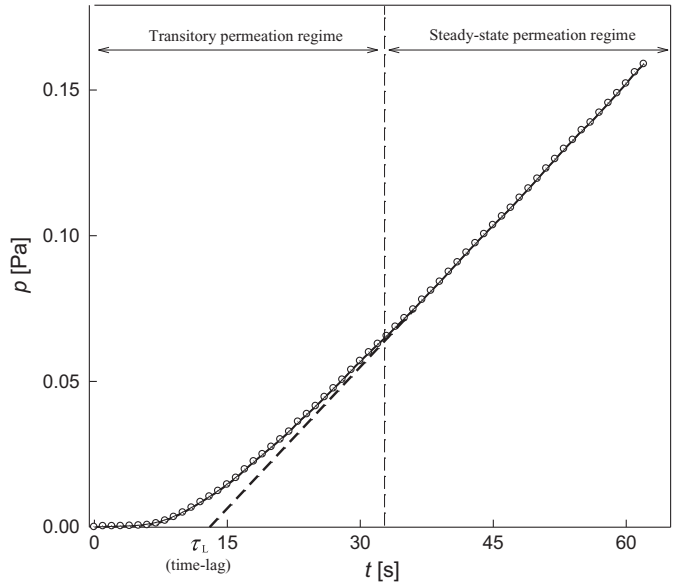

Fig. 2. Typical experimental permeation curve (FePC, $p_h = 1.5$ bar, $T = 475$ °C): transitory permeation regime, steady-state permeation regime and definition of the time lag τ_L.

(99.9999%), UHV state is reached inside the rig (up to 10^{-7} Pa) and, therefore, the absence of any oxygen, water vapor or any other deleterious species that may provoke surface oxidation of the specimen (S) can be assured.

4. Theory

The transport of hydrogen through the material can be limited by the interstitial diffusion of the gas through the bulk of the material or by the physical–chemical reactions that can take place in the surface, apart from the interaction with dislocations, grain boundaries and impurities of the alloy [18]. The objective of this work is to characterize permeability (Φ) of hydrogen under diffusion-limited regimes, where the transport parameters that define transport of hydrogen through the tested samples are the diffusivity (D_{eff}), the permeability (Φ) and the Sieverts′ constant [19]. These parameters are evaluated for each temperature (T_{eff}) and loading pressure (p_h). In order to get these values, the pressure increase in the low-pressure region due to the permeated flux is experimentally recorded. A non-linear least-squares fitting to the experimental data is then carried out. The theoretical expression for the pressure increase during time, $p(t)$, is obtained solving Fick′s second law and gives [20,21]:

$$p(t) = \frac{R \cdot T_{eff}}{V_{eff}} \left[\frac{\Phi \cdot {p_h}^{1/2}}{d} A \cdot t - \frac{\Phi \cdot {p_h}^{1/2} \cdot d}{6 D_{eff}} A - \frac{2\Phi \cdot {p_h}^{1/2} \cdot d}{\pi^2 D_{eff}} A \sum_{n=1}^{\infty} \frac{(-1)^n}{n^2} \exp\left(-D_{eff} \frac{n^2 \pi^2}{d^2} t \right) \right] \quad (1)$$

where, d is the thickness of the specimen, A the specimen area exposed to the gas volume, R is the ideal gas constant (8.314 J K^{-1} mol^{-1}), V_{eff} is the effective volume where the permeated gas is retained and T_{eff} is the temperature of the volume. The volume V_{eff} is precisely measured in each experimental permeation test by performing gas expansion to a calibrated volume. The first two addends inside the bracket provide important information of the steady-state permeation regime whereas the third addend is responsible for the definition or the transitory permeation regime.

When considering a very large period of time ($t \to \infty$), Eq. (1) shows the evolution of pressure with time for the steady-state permeation regime:

$$p(t) = \frac{R \cdot T_{eff}}{V_{eff}} \left[\frac{\Phi \cdot {p_h}^{1/2}}{d} A \cdot t - \frac{\Phi \cdot {p_h}^{1/2} \cdot d}{6 D_{eff}} A \right] \quad (2)$$

This expression corresponds to the steady-state flux observed in Fig. 2 as a linear tendency on the right-hand side. When the straight line is extended down to cross the abscise axis in the time co-ordinate a characteristic time known as time-lag is obtained:

$$\tau_L = \frac{d^2}{6 D_{eff}} \quad (3)$$

The value of the permeability, Φ, can be derived from the slope of the straight line in the steady-state permeation regime (Fig. 2, Eq. (2)) and the diffusivity (D_{eff}) can be derived from the value of the time lag (Fig. 2, Eq. (3)). Nevertheless, a non-linear least-squares fitting to all the experimental points of each single test has been preferred with the general expression given by Eq. (1) in both the steady-state region and the transitory region. When the experimental points recorded for one test fit the theoretical equation, results obtained for the transport parameters turn out to be more reliable. In any case, the non-linear least-squares fitting and the direct calculation of the transport parameters with the slope of the straight line and the time-lag, produced very similar results, which is a good indicator of the accuracy of the method. The Sieverts′ constant ($K_{S,eff}$) can be derived from the quotient of the previous transport parameters:

$$K_{S,eff} = \Phi / D_{eff} \quad (4)$$

The studied transport parameter in this work is the permeability (Φ). This parameter relates the flux of the gas in the steady-state regime (J) through one slice of the material defined by its thickness (d), due to the pressure difference between the opposite surfaces of the slice (p_1 and p_2). Under steady-state regime, diffusion-limited flux is described by Richardson′s law:

$$J = \frac{\Phi}{d} (p_1^{1/2} - p_2^{1/2}) \quad (5)$$

The permeability shows an Arrhenius type dependency with the absolute temperature T:

$$\Phi(T) = \Phi_0 \cdot \exp\left(\frac{-E_\Phi}{RT} \right) \quad (6)$$

where E_Φ is the permeation activation energy. Analogously, diffusivity and Sieverts′ constant show analogous Arrhenious tendencies.

5. Results and discussion

More than 60 individual permeation tests were carried out with each one of the six samples described before. The temperature range was from 423 K to 823 K and loading pressures from 1.0×10^3 Pa to 1.5×10^5 Pa. In all cases, a diffusion-limited regime was confirmed for the tested experimental ranges of pressures and temperatures by means of the analysis of the proportionality of the steady-state flux to the square root of the loading pressure, which is characteristic of diffusion-limited regime. As an example Fig. 3 shows these proportionalities for the FeCP alloy, where the powers obtained ($J \propto {p_h}^{0.5}$) were in the range from 0.505 to 0.598, with an average value of 0.556. The rest of the alloys show similar values for the aforementioned powers which indicates a diffusion-limited permeation regime [22]. The verification of the diffusion-limited regime does not imply that surface effects do not appear. In fact, the surface condition may affect significantly the processes of hydrogen permeation [23]. Nevertheless, in this case, once the steady

Please cite this article as: I. Peñalva et al., Influence of the C content on the permeation of hydrogen in Fe alloys with low contents of C, Nuclear Materials and Energy (2016), http://dx.doi.org/10.1016/j.nme.2016.02.004

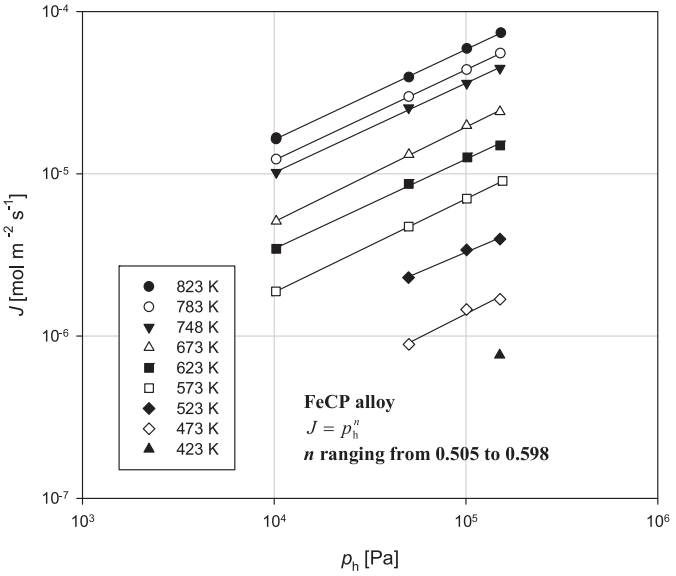

Fig. 3. Experimental hydrogen permeation steady-state flux in FeCP alloy: confirmation of diffusion limited regime ($J \propto p_h^{0,5}$) with experimental powers that are in the range from 0.505 to 0.598.

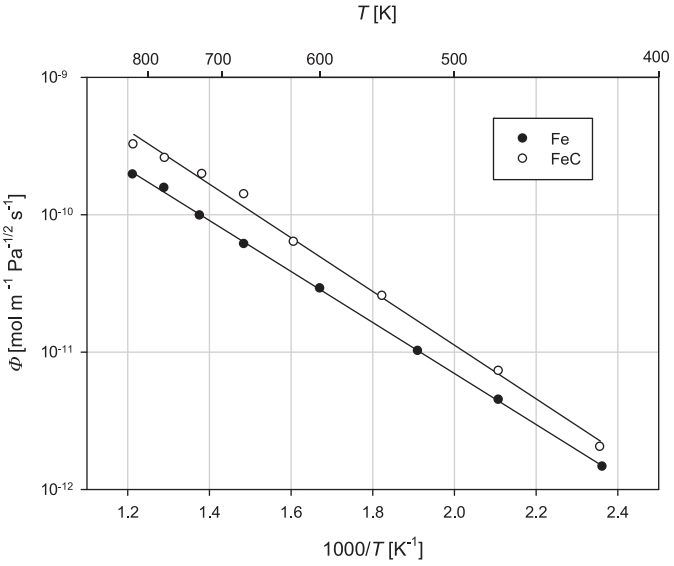

Fig. 4. Arrhenius plot of the fitted permeability of pure Fe and FeC alloys for the highest loading pressures at each temperature.

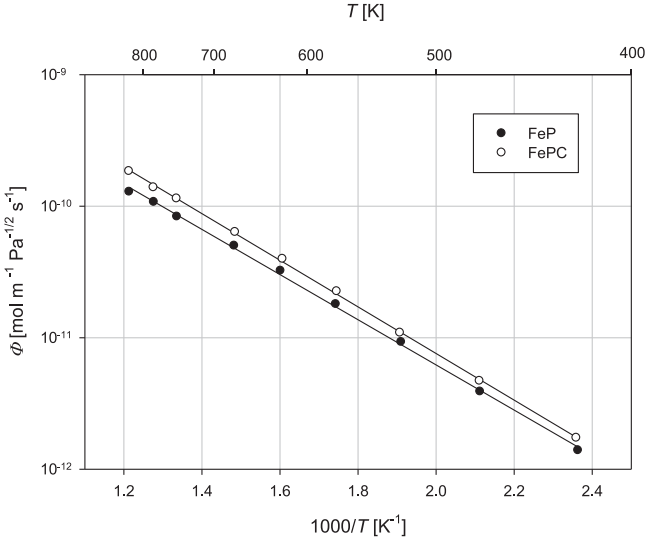

Fig. 5. Arrhenius plot of the fitted permeability of FeP and FePC alloys for the highest loading pressures at each temperature.

state regime is achieved, the flux rate of hydrogen that permeates through the sample turns out to be limited by diffusion in the bulk of the material.

The non-linear least-squares fitting of the experimental curves carried out for every permeation test (different loading pressures and temperatures in each case), lead to the calculation of the permeability. As expected (Eq. (6)), these values showed an Arrhenius type dependency with temperature. Table 2 summarizes the corresponding preexponencial values and the activation energies for permeability [14-16]. These results are also shown graphically in Figs. 4–6. Additionally, values for diffusivity and Sieverts´ constant are also provided in Table 2.

The comparison between the results obtained for the pure Fe alloy and the FeC alloy is the direct way to analyze the influence of C in the transport parameters without taking into account the synergistic effects caused by the presence of P and Cr. According to the results with these two alloys, permeation activation energies for both samples are similar with a small increase of the permeation prefactor for the FeC alloy. Fig. 4 shows this increase of the permeability due to the presence of low content of C for the highest loading pressures (typically $p_h = 1{,}5 \times 10^5$ Pa) at each temperature. These results are in good agreement with data shown in literature [12–16]: the permeation activation energy is not affected but addition of very low contents of C increases slightly the permeability; then, this tendency is inverted and permeability decreases as C content is increased [13]. The interaction of H with the bulk material seems to be slightly affected by the presence of low contents of C. This could be due to the direct interaction of H with C or with traps generated in the lattice by the addition of C to the alloy. Regarding diffusivity, the small thickness of the FeC alloy sample (see Table 1) led to an immediate transition to the steady-state regime and, therefore, the transitory regime could not be characterized.

The effects caused by the presence of P and Cr together with C can be analyzed comparing the results of FeP versus FePC and Fe10%Cr versus Fe10%CrC, respectively. In the first case, we observed a small increase of the permeation for the alloy containing

Table 2
Experimental permeability of hydrogen for the tested alloys.

Material	Φ_0 [mol m^{-1} Pa$^{-0.5}$ s^{-1}]	E_Φ [kJ mol^{-1}]	D_0 [m^2 s^{-1}]	E_D[kJ mol^{-1}]	K_{S0} [mol m^{-3} Pa$^{-0.5}$]	E_S[kJ mol^{-1}]
Pure Fe	3.11×10^{-8}	35.1	7.28×10^{-9}	1.3	4.27	33.8
FeC	6.87×10^{-8}	37.1	–	–	–	–
FeP	5.82×10^{-9}	26.5	2.49×10^{-8}	6.2	2.34×10^{-1}	20.3
FePC	2.32×10^{-8}	33.6	4.95×10^{-8}	9.1	4.69×10^{-1}	24.5
Fe10%Cr	3.46×10^{-8}	39.7	1.30×10^{-7}	14.4	2.66×10^{-1}	25.3
Fe10%CrC	5.56×10^{-8}	41.9	4.41×10^{-8}	9.7	1.26	32.2

Please cite this article as: I. Peñalva et al., Influence of the C content on the permeation of hydrogen in Fe alloys with low contents of C, Nuclear Materials and Energy (2016), http://dx.doi.org/10.1016/j.nme.2016.02.004

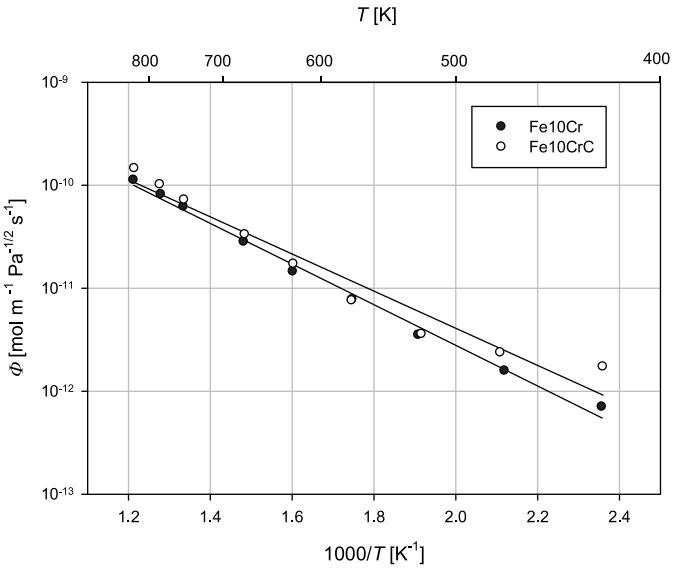

Fig. 6. Arrhenius plot of the fitted permeability of Fe10%Cr and Fe10%CrC alloys for the highest loading pressures at each temperature.

C in the whole region of temperatures that where tested (see Fig. 5). The same effect was observed when adding a similar small quantity of carbon (see Table 1) to the pure Fe sample. This seems to indicate that, regardless of the presence of P, the addition of small quantities of C lead to a slight increase of the permeability of hydrogen. Regarding diffusivity, it seems that there is not any significant influence when adding small quantities of C. Values are very similar in the whole region of temperatures that were tested.

On the other hand, when comparing the alloys containing Cr, we did not observe any increase of permeability when adding C (see Fig. 6). In general terms, the influence of the Cr content by itself is a subject of high importance and its influence has been extensively studied before [12–15]. Results obtained for permeability are in good agreement with these data. It seems that the influence of the C content is negligible in the case of alloys containing Cr, as long as the values obtained for the permeability remain almost the same in these samples for the whole range of temperatures, with only a slight deviation at lowest temperatures. According to these experimental results, the influence of the alloying element Cr seems to hide the effect of C in the case of permeability. However, the quantity of C added to the Fe10%CrC sample is much bigger than in the previous two samples (see Table 1). This bigger addition can lead to a different behavior in the crystal lattice. Small quantities of C would dissolve in the lattice, whereas addition of bigger quantities can lead to the formation of carbides [24]. These carbides would be responsible for the decrease of the permeability with increasing quantities of C, which is documented in literature [13]. Therefore, after a slight increase of the permeability due to the presence of some tens of ppm in weight of C in Fe alloys, additional increases of quantities of C would lead to smaller values of the permeability. In our case, regardless of the presence of Cr, we observed a negligible effect on the permeability when adding 820 ppm of C in weight. In this case, the effect on diffusivity was also insignificant.

6. Conclusions

The gas permeation technique was used to study the influence of the C content in the permeability of hydrogen by means of six Fe alloys provided by EFDA with controlled chemical alloying elements and microstructure. The steady-state permeation fluxes were analyzed for every test and a diffusion-limited regime was confirmed for all the samples. The values of the permeability (Φ) were experimentally measured for every individual test and, as a result, an Arrhenius type dependency with temperature of the permeability was calculated for every sample.

According to the results, the effect of the C content on the permeability of hydrogen in Fe alloys was analyzed. A slight increase of the permeability due to the presence of very low content of C was experimentally measured. The effects caused by the presence of P and Cr together with C were also studied, showing a negligible influence in the permeability of H due to the addition of low contents of C.

Acknowledgment

This work has been carried out in the framework of research projects funded by the Spanish Ministry of Science and Innovation (MEC08/98), the University of the Basque Country (UPV/EHU-EHU08-34) and the European Fusion Development Agreement (EFDA MAT-REMEV). The authors would also like to thank the FEMaS Coordinated Action project for the support in knowledge exchange among different research groups and Pilar Fernández from CIEMAT for the preparation of the tested samples.

References

[1] K. Ehrlich, S. Kelzenberg, H.-D. Röhrig, L. Schäfer, M. Schirra, J. Nucl. Mater 212-215 (1994) 678–683.
[2] E. Serra, A. Perujo, G. Benamati, J. Nucl. Mater. 245 (1997) 108–114.
[3] G.A. Esteban, A. Perujo, K. Douglas, L.A. Sedano, J. Nucl. Mater. 281 (2000) 34–41.
[4] G.A. Esteban, A. Perujo, L.A. Sedano, B. Mancinelli, J. Nucl. Mater. 282 (2000) 89–96.
[5] K. Ehrlich, Fusion Eng. Des. 56-57 (2001) 71–82.
[6] B. van der Schaaf, F. Tavassoli, C. Fazio, E. Rigal, E. Diegele, R. Lindau, G. LeMarois, Fusion Eng. Des. 69 (2003) 197–203.
[7] E. Serra, G. Benamati, O.V. Ogorodnikova, J. Nucl. Mater. 255 (1998) 105–115.
[8] G. Veredas, J. Fradera, I. Fernández, I. Peñalva, L. Mesquida, J. Abellá, J. Sempere, I. Martínez, B. Herrazti, L. Sedano, Fusion Eng. Des. 86 (2011) 2365–2369.
[9] R. Sacristán, G. Veredas, I. Bonjoch, I. Peñalva, E. Calderón, G. Alberro, D. Balart, A. Sarrionandia-Ibarra, F. Legarda, Fusion Eng. Des. 89 (2014) 1551–1556.
[10] R.A. Causey, J. Nucl. Mater. 300 (2002) 91–117.
[11] M- Glugla, R. Lässer, L. Dörr, D.K. Murdoch, R. Haange, H. Yoshida, Fusion Eng. Des. 69 (2003) 39–43.
[12] A.D. Le Claire, Report AERE-R-10598 (1982).
[13] P. Jung, J. Nucl. Mater. 238 (1996) 189–197.
[14] I. Peñalva, G. Alberro, J. Aranburu, F. Legarda, J. Sancho, R. Vila, C.J. Ortiz, J. Nucl. Mater 442 (2013) S719–S722.
[15] I. Peñalva, G. Alberro, F. Legarda, R. Vila, C.J. Ortiz, Fusion Eng. Des. 89 (2014) 1628–1632.
[16] I. Peñalva, G. Alberro, F. Legarda, C.J. Ortiz, R. Vila, Fusion Eng. Des 98-99 (2015) 2058–2062.
[17] J. Le Coze, 2007, Procurement of pure Fe metal And Fe-based alloys with controlled chemical alloying element contents and microstructure, Final Report on Model Alloy Preparation, Armines Ecole Nationale Superieure des Mines, Saint Etienne, France
[18] I. Peñalva, G. Alberro, F. Legarda, G.A. Esteban, B. Riccardi, L. Collini, Copper Alloys, Early Applications and Current Performance-Enhancing Processes, InTech, Rijeka, 2012, pp. 31–48.
[19] S. Alberici, S. Tominetti, Hydrogen Transport Parameters in Metal Lattices: a Comparison between Desorption and Permeation Measurement Techniques, ATI-Asssociazione Termotecnica Italiana-50th Congress, St. Vincent 1995.
[20] J. Crank, The Mathematics of Diffusion, Clarendon Press, Oxford, 1975.
[21] H.S. Carslaw, J.C. Jaeger, Conduction of Heat in Solids, 2nd edition, Clarendon Press, Oxford, 1959.
[22] G.A. Esteban, G. Alberro, I. Peñalva, A. Peña, F. Legarda, B. Riccardi, Fusion Eng. Des. 84 (2009) 757–761.
[23] G. Alefeld, J. Völkl, Hydrogen in Metals, Topics in Applied Physics 28 and 29, Springer-Verlag, Berlin Heidelberg, 1978.
[24] N.I. Medvedeva, D.C. Van Aken, J.E. Medved, Comp. Mater. Sci. 96 (2015) 159–164.